Data-driven temperature prediction and control methods for small biomass boiler heating system in northern China

Kai Wang[1], Yang Li[1], Zhimin Mu[2], Hong Pan[2], Wei Xu[3], Yongcheng Jiang[1*]

(1. *College of Engineering and Technology, Tianjin Agricultural University, Tianjin 300392, China*;
2. *College of Basic Science, Tianjin Agricultural University, Tianjin 300392, China*;
3. *College of Humanities, Tianjin Agricultural University, Tianjin 300392, China*)

Abstract: The small biomass boiler heating system (SBBHS) offers a cost-effective, convenient, safe, and environmentally friendly heating solution for small-scale users, providing notable social and economic advantages. Temperature prediction and control methods can enable SBBHS to operate more intelligently and autonomously, further minimizing heating expenses. This study focuses on a small biomass boiler heating system in Xinyang, Shandong, utilizing data-driven methods to analyze SBBHS performance in supply water temperature prediction and optimization. To achieve precise temperature predictions, an enhanced artificial neural network model is developed, trained, and validated, with the Levenberg-Marquardt optimization algorithm applied to adjust network weights and thresholds. Additionally, a feedback neural network is employed for short-term, 24-hour temperature predictions of the SBBHS. Experimental results demonstrate that this temperature prediction and control strategy ensures long-term indoor temperature stability and comfort while reducing heating costs. This research contributes to the intelligent upgrading and transformation of small biomass boiler control systems, enabling on-demand heating and reducing carbon emissions.
Keywords: neural network, biomass boiler, data-driven, temperature prediction, intelligent control
DOI: 10.25165/j.ijabe.20241706.9159

1 Introduction

Biomass, recognized as the fourth-largest energy source after coal, oil, and natural gas, is a form of chemical energy with properties similar to fossil fuels and holds significant potential as a renewable replacement without requiring modifications to existing energy infrastructure[1]. Biomass boilers, a type of energy equipment, can be categorized into biomass steam boilers, biomass hot water boilers, biomass hot air stoves, and biomass heat-conducting oil stoves[2]. The biomass boiler used in this study has gained popularity due to its high performance and potential for energy savings, emissions reduction, and economic benefits[3]. Goelles et al.[4] provided a comprehensive review of the history, current state, and future development trends of biomass fuel and biomass combustion boilers, proposing a heat transfer model for the convection section of a biomass boiler. Delubac et al.[5] introduced an innovative control method for a commercially available small-scale biomass boiler, significantly enhancing operational performance compared to conventional controls. Saidur et al.[6] compared the heating costs of biomass heating systems, fossil fuel systems, and electric heating systems, providing a cost analysis for residential heating applications.

A biomass boiler heating system harnesses biomass energy as its primary fuel, derived from renewable and abundant organic materials such as wood and agricultural residues. These systems are versatile, finding application across residential buildings, commercial properties, and industrial facilities. Serving as a renewable, environmentally friendly, and cost-effective alternative to traditional fossil fuel-based heating, biomass boiler systems utilize locally sourced fuel and produce minimal greenhouse gases, making them an ideal solution for sustainable heating. Currently, biomass boilers are still emerging on a relatively small scale. In small enterprises and family-operated workshops, limited energy-saving awareness and varying skill levels among management personnel often result in low combustion efficiency and energy waste[7]. Presently, boiler management primarily focuses on the boiler body, or source end, where heat is generated. The boiler operator adjusts settings based on readings from various meters at the heat user side (loading end), but feedback is often delayed. Without timely feedback from the loading end, operators may struggle to make prompt adjustments, leading to either energy waste or suboptimal heating quality. Establishing a comprehensive heating model that encompasses both the source and loading ends could provide valuable guidance for more effective biomass boiler management and operation.

As an advanced intelligent modeling method, neural networks offer robust nonlinear fitting capabilities, parallel information processing, and self-learning properties, distinguishing them from traditional models. These attributes include self-learning, self-organizing, adaptability, strong generalization, and the capacity to generate objective, reliable results. Neural networks establish relationships between input and output data through learning,

making them highly applicable in nonlinear system modeling prediction[8,9]. For instance, Li et al.[10] employed an improved BP neural network algorithm to predict heat load, selecting external variables like temperature and wind power as independent inputs. Similarly, Ma[11] used the BP neural network for heating load modeling, leveraging time, day, and month cycles to predict future heating loads periodically. Jovanovic et al.[12] explored multiple neural network types, including feed-forward backpropagation neural networks (FFNN), radial basis function networks (RBFN), and adaptive neuro-fuzzy inference systems (ANFIS), demonstrating that all could accurately predict heating energy consumption for a university campus. Additionally, Kieltyka et al.[13] introduced an Intelligent Prediction System (IPS) based on neural networks, which has since been implemented for regional heat use prediction.

However, heating load, while essential, does not directly guide boiler management in biomass boilers, which, due to their relatively recent development, still rely heavily on manual operation. As such, heating load data may not be directly actionable for boiler operators. Outdoor temperature fluctuations, particularly during the heating season, have a significant impact on supply and return water temperatures, directly influencing both heat energy efficiency and indoor thermal comfort[14]. Additionally, indoor temperature exerts a clear influence on heating load, with a generally inverse relationship between heating load and room temperature fluctuations, as the latter is a primary determinant of heating demand due to its perceptibility[15]. Thus, developing a model that incorporates a range of parameters, including outdoor temperature, heating water temperature, and indoor temperatures in rural households, can provide more actionable and effective guidance for biomass boiler management and operation.

In this study, the BP neural network functions as the heating model for both the source and loading ends, with temperature as the primary forecasting target rather than heat load. Parameters include outdoor-related temperature data, heating water temperature, and room temperature. The data underwent preprocessing, including outlier removal and normalization, and was filtered based on correlation and *p*-values. To improve the BP neural network's accuracy in predicting the loading end temperature, the model was optimized within the empirical formula range by varying the number of hidden layer nodes. The performance of different hidden layer configurations was tested and analyzed, and the BP neural network structure with the highest accuracy and optimal performance was selected. This optimized BP neural network model then predicted the water supply temperature for the next 24 hours, offering a quality evaluation of the heating system. These results provide an effective reference for boiler managers, helping to minimize energy loss at the source end while ensuring the heating quality for end users.

2   Materials and methods

2.1   Data collection

The data utilized for model establishment primarily originates from sensors and official meteorological bureau records. Huaniuwang village in Shangdian, Xinyang County, Shandong Province, was chosen as the project and experimental site, with data collected from January 1 2022, to March 1 2022. Local outdoor temperature, wind speed, and wind direction data were provided by the China Meteorological Administration for Xinyang County. Temperature data for supply and return water was collected from sensors positioned at the midpoint of the boiler's supply and return

water pipelines. To assess heating quality for rural households, data was taken from the household with the lowest heating performance. Following the JGJT132-2009 standard for residential building energy-saving assessment, temperature sensors were installed in central indoor locations on walls with heating pipes, ensuring no exposure to light or drafts. These sensor readings were taken as room temperature measurements. Due to variations in villagers' living habits and requirements, there were discrepancies between actual conditions and standardized testing. Factors such as wall materials and building structure[16-18] also affected individual room temperatures; however, these variables remained constant throughout the data collection and were not included as alternative input variables. Data from both the source and loading ends were uploaded to a cloud platform via Internet of Things (IoT) technology, with a recording frequency of 5 min for further analysis.

After due consideration of the delay in the heating system, hot water circulated in the village through pipes for 1 h. Temperature, a slower-changing variable floating by roughly 1°C in 1 h, was recorded and officially released every hour. See the data in Table 1.

Table 1   Part of data for Xinyang County, Shandong Province

Supply temperature/ °C	Returning water temperature/ °C	Outdoor temperature/ °C	Outdoor relative humidity/ %	Direction/ (°)	Room temperature/ °C	Wind power/ Grade
47.2	38.8	−6	87	73	19.8	1
47.1	38.9	−7	90	304	19.4	1
46.9	38.8	−7	92	257	19.2	1
46.6	38.4	−7	92	276	18.8	1
46.3	38.4	−8	91	180	18.8	0
46.8	39.0	−6	49	242	19.5	1
46.8	38.9	−7	56	317	19.3	1
46.5	39.0	−6	47	291	19.1	2
46.3	39.0	−6	47	263	18.7	1
46.0	38.7	−8	54	313	18.5	1
45.9	38.7	−8	55	299	18.2	1
45.2	38.1	−9	72	278	17.9	1
45.3	37.7	−10	70	261	18.0	1
44.5	36.8	−9	61	295	19.3	1
44.6	36.9	−5	42	354	19.8	2
45.8	38.1	−2	39	32	20.0	2

2.2   Data preprocessing

Due to factors such as equipment malfunction, human error, device precision limitations, data transmission interference, and adverse weather conditions[19], some data exhibited errors and reduced reliability. In this study, outlier removal and normalization methods were applied to reduce error rates and enhance data credibility. During the data processing phase, issues such as data upload failures and access irregularities on the cloud platform necessitated the removal of affected records. Additionally, fluctuating water levels in the pipeline contributed to data instability due to sensor placement, occasionally resulting in abnormally low values, as illustrated in Figure 1. Where, the red line represents the median, while the blue line indicates the mean. The top and bottom edges of the box correspond to the 75th percentile (Q3) and 25th percentile (Q1), respectively, with the maximum and minimum values positioned outside the box. Independent points beyond these boundaries are classified as outliers. Both supply and return water temperatures displayed outliers. The box length, calculated as the interquartile range (IQR) using the formula (IQR=Q3–Q1), defines

the interval for outlier detection. Minimum (min) and maximum (max) values were determined using (min=Q1–1.5×IQR) and (max=Q3+1.5×IQR). These bounds were used as thresholds for identifying and excluding outliers from the dataset.
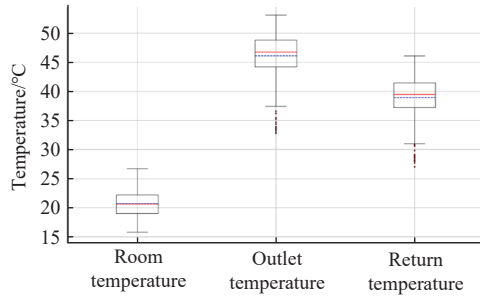
Note: The red line represents the median; the blue line indicates the mean.

Figure 1　Diagram of supply and return water and household room temperature box

Data normalization and inverse normalization are techniques used to transform dimensional data into a dimensionless range, typically between 0 and 1. This transformation accelerates network learning by reducing the mean of input signals for all samples, bringing it closer to zero or to a smaller value relative to its mean square error. Normalization also addresses issues of slow convergence and extended training time in neural networks caused by large data variation ranges[20]. Once input data is normalized, it must undergo inverse normalization to revert to its original dimensional values. The input and output variables are normalized according to Equation (1).

$$Y = Y_{min} + \frac{Y_{max} - Y_{min}}{X_{max} - X_{min}}(X - X_{min}) \tag{1}$$

where, Y_{max} and Y_{min} are the maximum and minimum data in the data set, respectively. Y is the normalized value of the original data, and X is the unprocessed value. X_{max} and X_{min} represent the maximum and minimum values in the data group for processing.

2.3　BP neural network

The BP neural network, also known as the error backpropagation network, is among the most widely used artificial neural networks. It operates with a "supervised" learning mode, characterized by strong learning capabilities, robust nonlinear mapping, and high fault tolerance[10]. With a suitable data sample, it effectively establishes associations between input and output variables[21]. Structurally, the BP neural network[22] comprises an input layer, a hidden layer, and an output layer. As illustrated in Figure 2, its learning process involves two main steps: forward transmission of input information and backpropagation of error information. During forward propagation, the input signals pass through the hidden layer and reach the output layer, where the mean square error is calculated. If the mean square error exceeds the acceptable threshold, backpropagation initiates, transferring errors sequentially from the output layer to the hidden layer, and finally to the input layer. This process involves iterative adjustments of weights and biases between layers, specifically from the hidden layer to the output layer, and from the input layer to the hidden layer. Input variable parameters are repeatedly trained until the mean square error meets the target threshold, ensuring accuracy in network learning.

2.4　Establishment and optimization of neural network structure

In this study, the nntool toolbox in MATLAB software was employed to construct the heating model for both the source and loading ends of the biomass boiler. When determining the number of nodes in the output layer, a comprehensive and extensive selection of variables was prioritized, followed by data analysis and other screening methods to test the variables, ultimately establishing the optimal node count[23]. For the hidden layer, the BP neural network's capacity to approximate any continuous nonlinear function with a single hidden layer was leveraged[24]. Therefore, a single hidden layer was prioritized in the network design to achieve model accuracy, as increasing the number of hidden layer nodes can reduce error[25-28]. This single hidden layer configuration was adopted to achieve optimal fitting within the model.
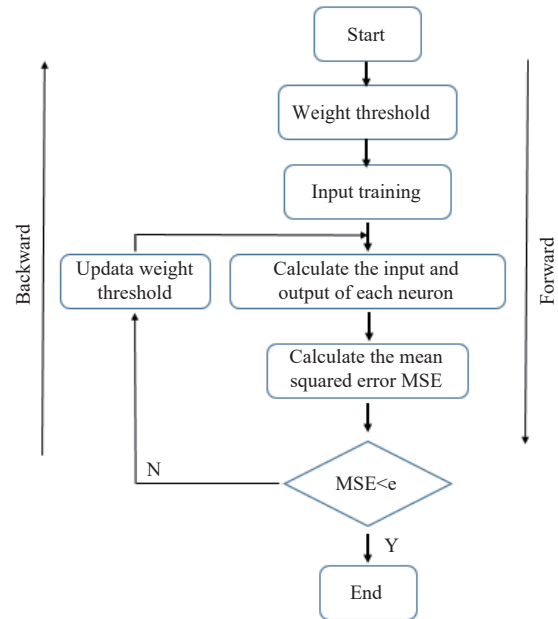
Figure 2　Diagram of BP neural network training process

The primary challenge in configuring the BP neural network lies in selecting an appropriate number of hidden layer nodes. An excessive number of hidden nodes may lead to an overly complex network structure, potentially resulting in overfitting, reduced fault tolerance, weakened generalization, and diminished processing capability. Conversely, too few hidden nodes produce an overly simplified structure, which may prevent adequate learning of input information and negatively impact the training outcomes[29]. To determine the optimal number of hidden layer nodes, the BP neural network employs an empirical formula, as shown in Equation (2).

$$N_h = \sqrt{N_{in} + N_{out}} + n \tag{2}$$

where, N_h represents the number of nodes in the hidden layer, N_{in} represents the number of nodes in the input layer, and N_{out} represents the number of nodes in the output layer, while n serves as an adjustable parameter typically ranging from 1 to 10, allowing for fine-tuning of hidden layer node counts.

During the training phase of the neural network, the choice of training algorithm plays a critical optimization role. This study employs the Levenberg-Marquardt algorithm, known for its rapid convergence and ability to mitigate the common issues of the BP algorithm, including susceptibility to local minima and slow convergence[30]. Additionally, the learning rate selection is typically experience-based, as it is challenging to determine through specific methods[25].

2.5　Evaluation and test of BP neural network model

After establishing the BP neural network model, factors such as

unknown information, missing input variables, and numerous uncontrollable influences may introduce inevitable errors between the model's predictions and actual values. The BP neural network's training process primarily focuses on adjusting parameters to minimize the mean square error (MSE) to meet the target accuracy. As shown in Equation 3, the MSE is a critical metric for model evaluation.

$$MSE = \frac{1}{n} \sum_{i=1}^{n} (Y_i - \hat{Y}_i)^2 \qquad (3)$$

where, n represents the dataset length, Y denotes the actual household temperature data, and $\hat{Y}$ represents the predicted household temperature data. Additionally, the correlation coefficients between the training, test, validation, and overall datasets and their corresponding prediction sets serve as important indicators for assessing the network model's performance.

3   Results and analysis

3.1   Analysis of input variable

The collected data included several candidate variables for input, such as supply water temperature, return water temperature, outdoor temperature, wind direction, and wind speed. The final input variables for modeling were selected based on the correlation and p-values between these candidate variables and the output variable, room temperature.

As listed in Table 2, supply water temperature, return water temperature, and outdoor temperature exhibit a strong correlation with room temperature and possess very low p-values, indicating their suitability as input variables. However, since this model is primarily designed for management purposes, return water temperature, which cannot be obtained in advance for forecasting, was excluded as an input variable. Although wind speed has a weak correlation with room temperature, its low p-value justifies its inclusion as an input variable. Conversely, wind direction and outdoor relative humidity, with low correlations and high p-values, were excluded from the model as input variables.

Table 2   Correlation and significance between different data and room temperature

Data matching name	Correlation	The value of p
The supply temperature and room temperature	0.6110	≪0.002 00
Returning water temperature and room temperature	0.6690	≪0.002 00
Wind power and room temperature	0.2893	≪0.002 00
Wind direction and room temperature	−0.0218	0.611 67
Outdoor temperature and room temperature	0.7476	≪0.002 00
Outdoor relative humidity and room temperature	−0.1932	0.000 01

3.2   Establishment and performance evaluation of BP neural network model

Parameter selection is essential for establishing an effective neural network model. Based on the empirical formula for determining the number of hidden layer nodes in a BP neural network: Equation (2), the input layer consists of 3 nodes, and the output layer contains 1 node. Therefore, the number of nodes in the hidden layer should range between 3 and 12. Various models were trained using BP neural networks with different numbers of hidden layer nodes. A learning rate of 0.001 was applied for optimal fitting.

As listed in Table 3, the model with 3 hidden layer nodes exhibited the highest mean square error, while the model with 11 hidden layer nodes achieved the lowest mean square error. Examining the correlation coefficient between the entire dataset and

its corresponding prediction set, the model with the highest correlation contained 12 hidden layer nodes, and the one with the lowest correlation contained 3 nodes. Notably, the correlation does not increase linearly with the number of hidden layer nodes. Consequently, the model that achieved both the minimum mean square error and a high correlation coefficient was selected as the source and loading end heating model for the biomass boiler, according to the performance criteria. In this study, the optimal BP neural network configuration includes 11 hidden layer nodes.

Table 3   Performance of models with different hidden nodes

Number of hidden layer nodes	MSE	Training correlation	Verify dependencies	Test correlation	All relevance
3	1.115 20	0.879 91	0.866 63	0.858 11	0.874 80
4	1.018 20	0.888 41	0.895 34	0.873 14	0.887 40
5	0.866 27	0.879 95	0.914 14	0.880 02	0.884 96
6	0.930 56	0.888 14	0.889 78	0.907 60	0.891 70
7	0.879 40	0.894 09	0.888 08	0.885 95	0.892 43
8	0.927 72	0.897 40	0.905 80	0.875 53	0.895 37
9	0.990 75	0.884 08	0.899 40	0.867 59	0.884 40
10	0.912 84	0.899 23	0.876 02	0.865 13	0.891 86
11	0.833 60	0.893 64	0.890 80	0.871 57	0.889 65
12	0.895 63	0.867 62	0.902 53	0.872 62	0.895 59

The BP neural network model, depicted in Figure 3, is configured with eleven hidden layer nodes, three input variables, one output variable, and uses a sigmoid activation function in the hidden layers. In Figure 4, which illustrates the mean square error (MSE) performance, the x-axis represents the number of BP neural network iterations, while the y-axis represents the MSE. The three curves shown correspond to the mean square error of the training set, validation set, and test set, respectively. The iteration count that achieves the closest value to the optimal (Best) mean square error occurs at the 8th iteration.
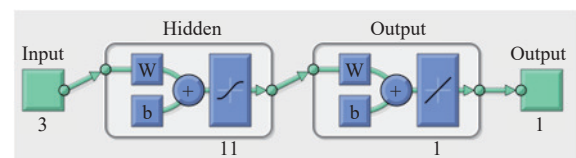
Figure 3   Structure of neural network
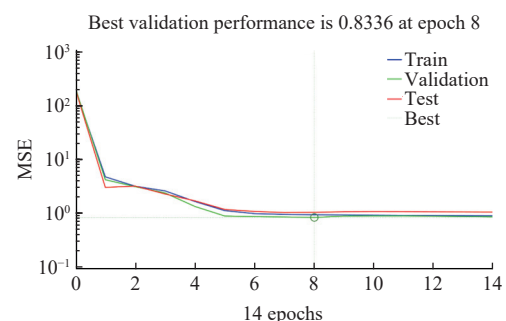
Figure 4   Trend of mean square error of each dataset

Furthermore, linear regression plots are generated to illustrate the relationship between the true values and their corresponding predicted values across various datasets, including the training set, validation set, test set, and the entire dataset (as depicted in Figure 5). The correlation coefficients for these relationships are found to be 0.893 64, 0.890 80, 0.871 57, and 0.889 65, respectively. Notably, a majority of data points are closely clustered

around the $Y=T$ dotted line with minimal deviation from it as indicated by small angles with the fit line. These findings suggest that the neural network model established in this study exhibits excellent performance with high accuracy.
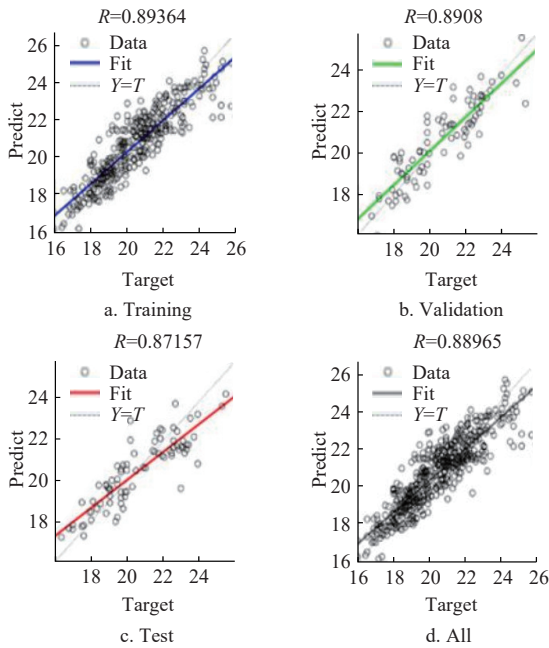
Figure 5   Goodness of fit between true and predicted values

3.3 The management of supply water temperature based on prediction model

The objective of boiler regulation and management is to ensure an appropriate supply water temperature that meets indoor temperature requirements. To control the boiler's supply water temperature, a pre-simulation approach based on the proposed model was adopted, with the corresponding flowchart illustrated in Figures 6-10.
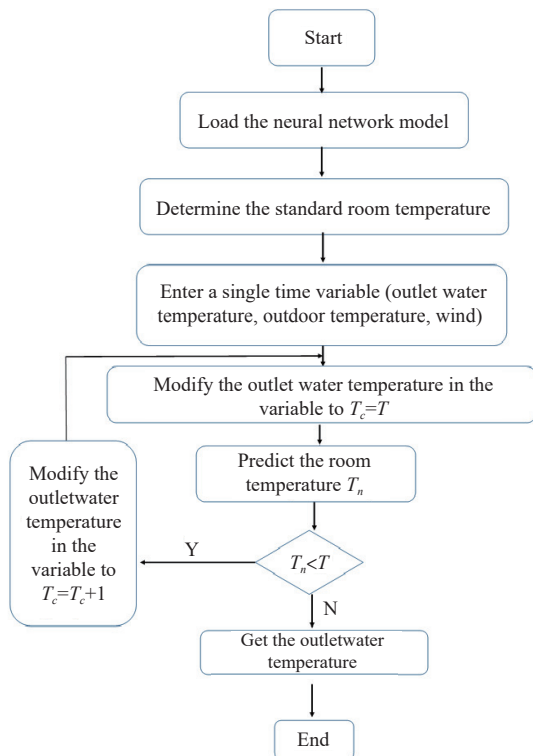
Figure 6   Flow diagram of model prediction at a single time

According to the Indoor Air Quality Standard (GB/T18883-2002), the recommended winter indoor temperature ranges from 16°C to 24°C, considered a comfortable temperature range. Due to significant heat losses, the minimum supply water temperature (input variable) must exceed either 16°C or 24°C to achieve an indoor temperature of 16°C or 24°C for rural households. As shown in Figure 6, after the model is loaded, the room standard temperature T is set to 16°C or 24°C. A single variable (supply temperature, outdoor temperature, or wind speed) is input, and the supply temperature T_c is adjusted to meet the target room temperature T. Modified variables are then used for simulated predictions. If the predicted room temperature T_n is less than the standard temperature T, T_c is incremented by 1, and the simulation is repeated until $T_n \geq T$. This final T_c value is recommended as the supply water temperature.

With a standard room temperature of 16°C, the increasing trend of supply water temperature is illustrated in Figure 7, where the solid line represents the supply water temperature and the dotted line indicates the room temperature. The simulation cycle was conducted under conditions of wind speed 1, outdoor temperature –6°C, and an initial supply water temperature of 16°C. After 20 simulation cycles, the optimal supply water temperature was determined. When the supply water temperature reaches at least 34°C, the room temperature achieves or exceeds the standard of 16°C.
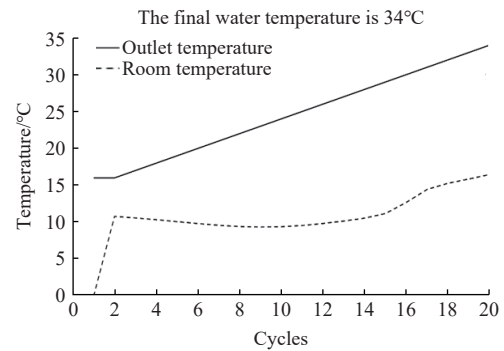
Figure 7   Increasing trend of supply water temperature with 16°C as the room temperature standard

Taking 24°C as the standard room temperature, the increasing trend of supply temperature is in Figure 8. The supply water temperature and room temperature are with the solid line and the dotted line, respectively. The cycle simulation was carried out under wind power 1, the outdoor temperature –6°C, and the supply temperature 24°C. The final supply temperature was obtained by 280 cycles. When the supply water temperature was at least 302°C, the room temperature could be greater than 24°C. However, the
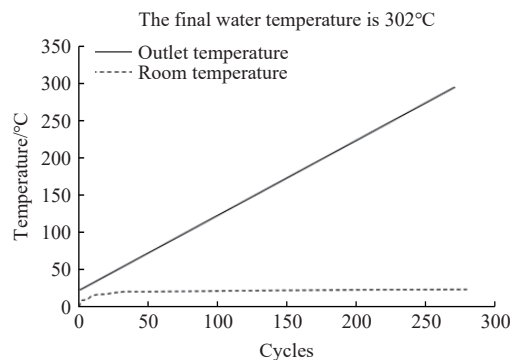
Figure 8   Increasing trend of supply water temperature with 24°C as the room temperature standard

continuous increase of supply water temperature has little influence on the change in room temperature. The supply water temperature of the biomass hot water boiler could not reach 302°C, so the room temperature could not be 24°C simply through heating of the boiler.

Through multiple simulations, it was determined that 21°C is the maximum achievable room temperature provided by the heating system under certain constraints. As shown in Figure 9, which illustrates the increasing trend of supply water temperature, the solid line represents the supply water temperature, while the dotted line indicates the room temperature. The simulation was conducted with wind speed 1, an outdoor temperature of –6°C, and an initial supply water temperature of 21°C. After 37 cycles, the optimal supply water temperature was identified. When the supply water temperature reaches at least 56°C, the room temperature can exceed 21°C.
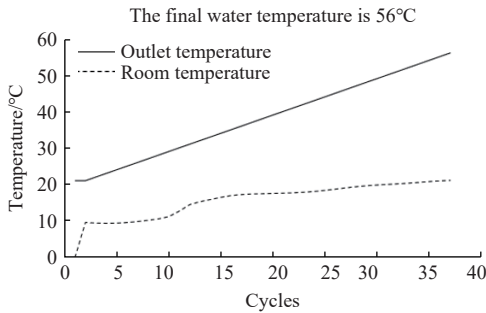
Figure 9   Increasing trend of supply water temperature with 21°C as the room temperature standard

The results of multi-time simulation predictions were consistent with those of single-time simulations. In Figure 10, after the model was loaded, the room standard temperature T was set to either 16°C or 24°C. In multi-time simulations, the variable sequence was input prior to each single-time simulation cycle. Individual variables were input sequentially, and the supply temperature T_c was adjusted to meet the room temperature standard T. After the simulation using the adjusted variables, the predicted room temperature T_n was compared to the standard room temperature T. If $T_n < T$, the model increased T_c by 1 and re-rank the simulation until $T_n \geq T$. The resulting value of T_c was recorded as the supply water temperature.

For each single variable input, T_c was adjusted and simulated until the room temperature T_n met or exceeded T. The supply water temperature T_c for each time point was stored in T_{clist} for the next round of single-time simulations. This process was repeated until the entire time series was simulated, yielding the complete supply water temperature sequence T_{clist}.

As required for next-day management, official 24-hour forecasts of outdoor temperature and wind speed from the local meteorological bureau can be input in advance. A 24-hour data sample from the actual dataset was selected to extract its outdoor temperature and wind speed as multi-time variable sequences. Using 21°C and 16°C as target room temperatures, the neural network model predicted room temperature with outdoor temperature and wind speed as the multi-time input sequence.

In Figure 11, two 24-hour supply water temperature curves are shown, representing the actual supply water temperature. The solid line and dotted line illustrate the lower-limit and upper-limit supply temperatures, respectively. The 24-hour supply water temperature curve, obtained from an indoor temperature simulation with a target of 16°C, is shown by the solid line, while the dotted line represents the upper-limit supply temperature curve based on a target room temperature of 21°C. Managers are advised to maintain supply water temperatures within these upper and lower bounds to achieve room temperatures between 16°C and 21°C, thus avoiding energy waste while ensuring adequate heating quality.
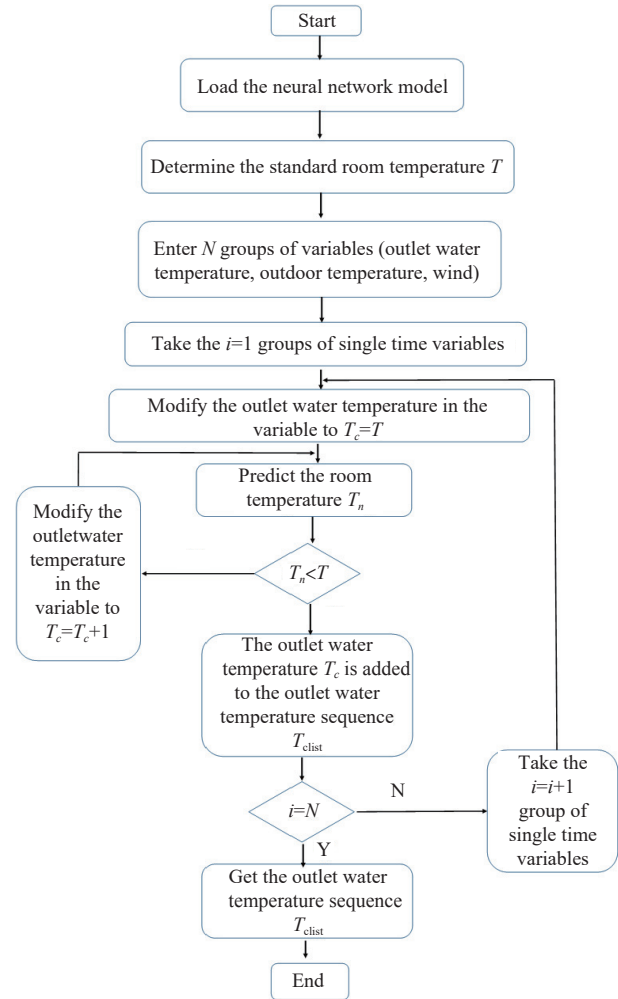
Figure 10   Flow diagram of model prediction at a multi-time
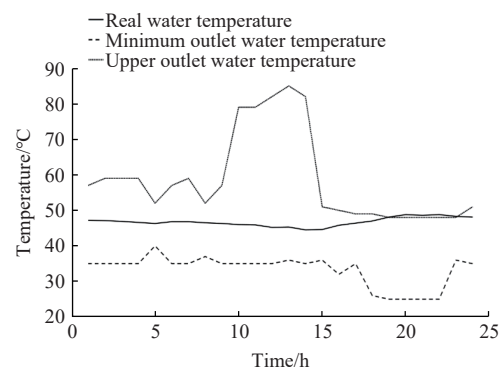
Figure 11   The upper limit and the lower limit of the supply water temperature in 24 h

The boiler heating quality is assessed during data acquisition using the model, which predicts and simulates supply water temperature. In Figure 12, the real water temperature is represented by the solid line, while the lower-limit and the upper-limit of outlet water temperature are indicated by different types of dashed lines. The simulated dashed curve, which represents the 24-hour supply water temperature, is based on a target room temperature of 16°C. The upper-limit outlet water temperature for a target room temperature of 21°C over the same period. Throughout this period,

most of the real supply water temperatures exceed the lower limit, with certain segments also slightly surpassing the upper limit. This suggests that there is some degree of energy waste within the heating system.
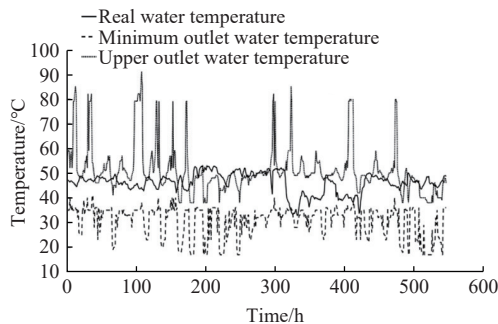
Figure 12   The upper limit and the lower limit of the supply water temperature during the heating experiment

In Figure 13, the x-axis represents operation time, while the y-axis indicates the household room temperature. The room temperature in this village generally exceeds the standard target of 16°C, although it tends to be slightly lower in households located toward the middle and end of the pipeline. This trend reflects the room temperatures experienced by most households in the village. Overall, the biomass boiler heating system is capable of providing high-quality heating for the majority of local users.
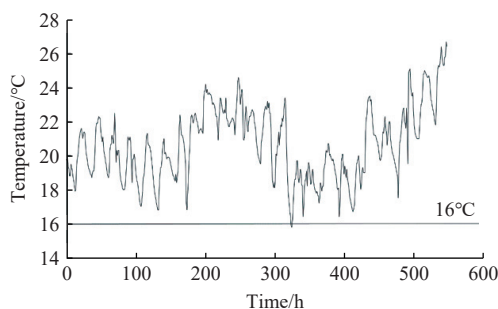
Figure 13   Curve of the room temperature of the household

4   Conclusions

Through correlation analysis between outdoor temperature, supply and return water temperatures, wind speed, wind direction, and outdoor relative humidity with peasant household room temperature, outdoor temperature, water temperature, and wind speed were identified as the primary factors affecting indoor temperature. Consequently, water temperature, outdoor temperature, and wind speed were selected as input variables for the neural network. Outliers were removed, and data normalization was applied to improve data quality.

A 24-h supply water temperature prediction for the SBBHS was achieved using actual measurements from the biomass boiler. The prediction utilized a feed-forward neural network with a backpropagation learning algorithm, achieving a mean square error (MSE) of 0.8336. Correlations for the training set, validation set, test set, overall predicted values, and actual values were 0.893 64, 0.890 80, 0.871 57, and 0.889 65, respectively.

The simulation results from the neural network predictions were compared with actual supply water temperature data from the biomass boiler, yielding satisfactory results with an acceptable average error. Future work will focus on strategies to further reduce the energy consumption of the biomass boiler system.

[References]

[1]   Du W, Wang J Z, Feng Y X, Duan W J, Wang Z L, Chen Y C, et. al. Biomass as residential energy in China: Current status and future perspectives. Renewable and Sustainable Energy Reviews, 2023; 186: 113657.

[2]   Wu W X, Li H S, Li Q, Kong F R. The development status of biomass boilers and its application in agriculture. Agricultural Equipment and Vehicle Engineering, 2018; 56(3): 81–84. (in Chinese)

[3]   Shao S, Chao Y W, Li X, Xi J Q. Comparative and analysis of economy between biomass fired boiler and traditional fossil fuel fired boiler. Forestry Machinery and Woodworking Equipment, 2022; 50(1): 68–70.

[4]   Dourdoumas N, Brunner T, Golles M, Reiter S, Obernberger I. Model based control of a small-scale biomass boiler. Control Engineering Practice, 2014; 22(1): 94–102.

[5]   Majchrzycka A. Comparative analysis of individual house heating system based on electricity and combustion of alternative and fossil fuels. Bulgarian Chemical Communications, 2016; 48: 242–247.

[6]   Saidur R, Abdelaziz E A, Demirbas A, Hossain M S, Mekhilef S. A review on biomass as a fuel for boilers. Renewable and Sustainable Energy Reviews, 2011; 15(5): 2262–2289.

[7]   Fan C L. Analysis of the status quo of biomass boilers. Chemical Management, 2016; 23: 4–5.

[8]   Jiao L C. Theory of artificial neural network. In Jiao L C, editor. Neural Network System Theory. Xi'an: Xidian University Press. 1990; pp 76–85.

[9]   Ding F J, Jia X D, Hong T J, Xu Y L. Prediction model on flow stress of 6061 aluminum alloy sheet based on GA-BP and PSO-BP neural networks. Rare Metal Materials and Engineering, 2020; 49(6): 1840–1853.

[10]   Li S Q, Jang Z J. Heating load prediction model based on improved BP neural network. Software Guide, 2019; 18(7): 41–44, 48. (in Chinese)

[11]   Ma Y Y. Research and implementation of online monitoring and management methods for heating systems. Master dissertation, Shenyang: Shenyang University of Technology, Shenyang, 2020; 64 p. (in Chinese)

[12]   Jovanović R Z, Sretenović A A, Živković B D. Ensemble of various neural networks for prediction of heating energy consumption. Energy and Buildings, 2015; 94: 189–199.

[13]   Kiełtyka L, Kuceba R, Sokolowski A. Application of neural network topologies in the intelligent heat use prediction system. Artificial Intelligence and Soft Computing, 2004; 3070: 1136–1141.

[14]   Yang X M, Meng Z Y, Wang F L, Xi W T, Liu T, Liu K. Influence of outdoor temperature changes in heating season on indoor supply and return water temperature and environmental thermal comfort. Cleaning and Air Conditioning Technology, 2019; 3: 31–34. (in Chinese)

[15]   Nagahara M. Convex optimization for sparse modeling. Systems, Control and Information, 2017; 61(1): 20–28. (in Japanese)

[16]   Kodah Z H, Jarrah M A, Shanshal N S. Thermal characterization of foam-cane(Quseab) as an insulant material. Energy Conversion and Management, 1999; 40(4): 349–367.

[17]   Femando B, Tadeu A, Simões N. Heat conduction across double brick walls via BEM. Building and Environment, 2004; 39(1): 51–58.

[18]   Herring H. National building stocks: Addressing energy consumption order carbonization. Building Research and Information, 2009; 37(2): 192–195.

[19]   Li J H. Application of terminal dynamic load forecasting in energy-saving control of central heating system. Master dissertation. Guangzhou: Guangzhou University, 2019; 64 p. (in Chinese)

[20]   Zhu Q S, Zhu D D, Huang W. BP neural network sample data preprocessing application research. World Science and Technology Research and Development, 2012; 34(4): 624–626. (in Chinese)

[21]   Rumelhart D E, Hinton G E, Williams R J. Learning representations by back-propagated error. Nature, 1986; 323: 533–536.

[22]   Bai S. Growing random forest on deep convolutional neural networks for scene categorization. Expert Systems with Applications, 2017; 71:

279–287.

[23] Zou H F, Xia G P, Yang F T. A neural network prediction model based on two-stage optimization algorithm. Journal of Management Science, 2006; 5: 28–35. (in Chinese)

[24] Tian Y, Jia Z Q, Yang X H. Improving shrub biomasses estimations in the Qinghai-Tibet Plateau: Age-based Caragana inter media allometric models. The Forestry Chronicle, 2014; 90(2): 154–160.

[25] Yu L H, Xie L Y, Liu C M, Yu S, Guo Y X, Yang K J. Optimization of BP neural network model by chaotic krill herd algorithm. Alexandria Engineering Journal, 2022; 61(12): 9769–9777.

[26] Hornik K, Stinchcombe M, White H. Universal approximation of an unknown mapping and its derivatives using multilayer feedforward networks. Neural Networks, 1990; 3(5): 551–560.

[27] Castro J L, Mantas C J, Benítez J M. Neural networks with a continuous squashing function in the output are universal approximators. Neural Networks, 2000; 13(6): 561–563.

[28] Ayyad M, Yang L S, Ahmed A, Shalaby A, Huang J, Mi J, et. al. System identification of oscillating surge wave energy converter using physics-informed neural network. Applied Energy, 2025; 378: 124703.

[29] Michalopoulos J, Papadokonstadakis S, Arampatzis G, Lygeros A. Modelling of an industrial fluid catalytic cracking unit using neural networks. Chemical Engineering Research and Design, 2001; 79(2): 137–142.

[30] Sun Q. Research and application of recommendation algorithm based on LM-BP neural network. Master dissertation, Beijing: Beijing Jiao Tong University, 2016; 69p.